Photoionization of resonantly driven atomic states by an extreme ultraviolet-free-electron laser: intensity dependence and renormalization of Rabi frequencies

2013 New J. Phys. 15 093016

(http://iopscience.iop.org/1367-2630/15/9/093016)

New Journal of Physics
The open access journal for physics

Photoionization of resonantly driven atomic states by an extreme ultraviolet-free-electron laser: intensity dependence and renormalization of Rabi frequencies

B Kaiser[1,3], A Brand[1], M Glässl[1], A Vagov[1], V M Axt[1] and U Pietsch[2]

[1] Institut für Theoretische Physik III, Universität Bayreuth, D-95440 Bayreuth, Germany
[2] Institut für Festkörperphysik, Universität Siegen, D-57068 Siegen, Germany
E-mail: benjamin.kaiser@uni-bayreuth.de

New Journal of Physics **15** (2013) 093016 (16pp)
Received 12 June 2013
Published 12 September 2013
Online at http://www.njp.org/
doi:10.1088/1367-2630/15/9/093016

Abstract. We analyze theoretically the high intensity photoionization dynamics of a system with two atomic states resonantly coupled by coherent extreme ultraviolet laser radiation that also gives rise to the ionization. The ground state occupation of such a system is shown to exhibit damped Rabi oscillations. The corresponding ionization, which is responsible for the damping, scales almost linearly with the field intensity when the pulse length exceeds the Rabi period. For shorter pulses a quadratic scaling is found. The Rabi frequency is shifted compared to its value for an isolated two-level system. The shift increases with excitation intensity and can acquire a high percentage of the unrenormalized frequency at high intensities. Analytical results obtained within a simplified solvable model demonstrate that the damping and the shift both result from the coupling of the discrete states to the ionization continuum and are therefore closely related. Numerical simulations for a two-electron system reveal at high intensities the importance of off-resonant ionization channels.

[3] Author to whom any correspondence should be addressed.

Contents

1. Introduction

The physics of matter in highly intense extreme ultraviolet (XUV) or x-ray radiation is profoundly different from the weak field limit as has been shown by demonstrating many fascinating properties occurring, e.g. in the ionization dynamics at strong fields [1–8]. Many of these phenomena can be described by rate equations, which are widely used in current publications [9–11]. However, this picture completely breaks down in strong laser fields with small bandwidths as demonstrated in pioneering works of Beers and Armstrong [12] and Knight [13], where coherent Rabi oscillations are shown to accompany the ionization dynamics. Such a scenario is also markedly different from the well known case of Rabi dynamics in an isolated two-level system, because due to the coupling to the continuum of ionized states, carriers can leave the resonantly coupled subsystem, which is reflected in a pronounced damping of the Rabi oscillations [13]. Rabi oscillations are, however, not the only signatures of coherent dynamics that affect the ionization process. For example, recent studies have revealed the impact of quantum interference effects on the ionization dynamics [14].

Driven by the availability of a new generation of free-electron laser (FEL) sources [15, 16], which deliver short pulses of unprecedented strength, the interest in studies of the impact of Rabi dynamics on ionization processes has recently been renewed. In H_2 molecules exposed to intense and ultrashort vacuum ultraviolet pulses, a step-ladder Rabi oscillation mechanism has been identified, that successively involves higher and higher vibrational states [17]. In [18] it has been demonstrated, that Rabi oscillations suppress the ionization probability in the resonant two-photon ionization of He by extreme ultraviolet FELs and multiphoton nonsequential double ionization of He atoms in intense laser fields at UV wavelength has been shown to be considerably affected by multiphoton Rabi oscillations [19]. Further, the impact of Rabi oscillations on the resonant Auger effect in Ne atoms has been studied theoretically [20–22] and recent experiments confirmed the predicted broadening of the Auger emission lines [23] for stochastically emitted pulses by self-amplified spontaneous emission (SASE).

In this paper we shall demonstrate that at strong coherent driving fields, which are accessible by seeding techniques [24], the frequency of the Rabi oscillations is considerably renormalized and the renormalization increases with rising field strength. The effect is shown to be due to the field induced coupling of the bound states to the continuum of ionization states. Thus, the frequency renormalization and the ionization have the same physical origin and are therefore closely related. Within a simplified analytically solvable model we shall make this

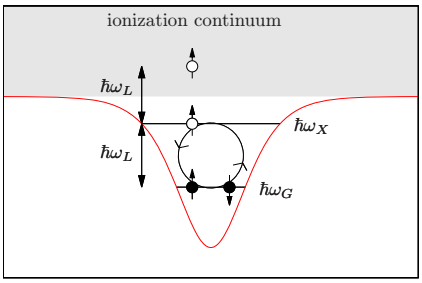

Figure 1. Schematic view of a system with two discrete states performing Rabi oscillations that compete with ionization processes. In this example, the lower state is initially occupied by two electrons that subsequently may either stay in the Rabi cycle with the resonantly driven upper discrete state or may escape into the ionization continuum.

relation explicit. Numerical studies based on a one-dimensional two-electron system serve to illustrate the analytically obtained conclusions and to discern the limits of the simplified model. It turns out that the ionization yield scales linearly with intensity as soon as the pulse length exceeds the Rabi period while for shorter pulses a quadratic scaling is found.

2. A generic model

A complete first principle theoretical modeling of atomic ionization dynamics is very difficult even for atoms with only few electrons. It is, therefore, important to reduce the full many-particle problem to a simpler easily tractable problem involving only a few most relevant components, which allows for a clear analysis of the main points. As the prime interest of this work is to study the dynamics of resonantly driven states where the ionization competes with coherent Rabi oscillations, we assume that the essential physics can be captured by a generic model, that is schematically illustrated in figure 1. The most important components of this model are two quantum states, $|G\rangle$ and $|X\rangle$, connected with the ionization continuum $|\omega\nu\rangle$ via the dipole coupling to the external monochromatic light field of frequency ω_{L} and with the amplitude E_0.

The model is defined by the Hamiltonian

$$H = H_0 + H_{\mathrm{Laser}} \tag{1}$$

with

$$H_0 = \hbar\omega_G|G\rangle\langle G| + \hbar\omega_X|X\rangle\langle X| + \int_0^\infty \mathrm{d}\omega \sum_\nu \hbar\omega|\omega\nu\rangle\langle\nu\omega|, \tag{2}$$

where the index ν accounts for possible degeneracies of the continuum states and $\hbar\omega_G$, $\hbar\omega_X$ and $\hbar\omega$ are the energies of the states $|G\rangle$, $|X\rangle$ and $|\omega\nu\rangle$, respectively. H_{Laser} represents the dipole coupling to an external laser field $\vec{E}(t)$. Here, we shall assume a monochromatic laser with frequency ω_{L} operating with a constant amplitude E_0 that is switched on at time $t = 0$, i.e.

$$\vec{E}(t) = \theta(t)\, E_0 \mathrm{e}^{-\mathrm{i}\omega_{\mathrm{L}}t}\, \vec{e}_{\mathrm{L}} + \mathrm{c.c.}, \tag{3}$$

where $\vec{e}_{\mathrm{L}}$ is the polarization vector of the laser field and $\theta(t)$ is the Heaviside function.

We consider a situation as sketched in figure 1 where two discrete levels are well separated from the ionization continuum and are driven resonantly while the laser energy $\hbar\omega_{\mathrm{L}}$ is sufficient to allow for a direct ionization from the upper level by a one photon process. Under these conditions and using resonance considerations it is reasonable to assume that the dipole couplings between the two discrete states as well as between the upper state and the continuum are more important than those between the ground state and the continuum or those within the continuum. Concentrating on the former and making use of the rotating wave approximation (RWA), which keeps only resonant contributions, the Hamiltonian for the dipole coupling reads

$$H_{\mathrm{Laser}} = \hbar\theta(t)\Big[E_0^*\mu_0^*\,\mathrm{e}^{\mathrm{i}\omega_{\mathrm{L}}t}|G\rangle\langle X| + E_0\mu_0\,\mathrm{e}^{-\mathrm{i}\omega_{\mathrm{L}}t}|X\rangle\langle G| + \int_0^\infty \mathrm{d}\omega \sum_\nu \left(E_0^*\mu_{\omega\nu}^*\,\mathrm{e}^{\mathrm{i}\omega_{\mathrm{L}}t}|X\rangle\langle\nu\omega| + E_0\mu_{\omega\nu}\,\mathrm{e}^{-\mathrm{i}\omega_{\mathrm{L}}t}|\omega\nu\rangle\langle X|\right)\Big], \tag{4}$$

where $\hbar\mu_0 = \vec{e}_{\mathrm{L}}\cdot\langle X|e\vec{r}|G\rangle$ and $\hbar\mu_{\omega\nu} = \vec{e}_{\mathrm{L}}\cdot\langle\omega\nu|e\vec{r}|X\rangle$ are the respective dipole coupling matrix elements with e being the electron charge. Similar models have been used for a long time for different purposes (see e.g. [12, 13, 25, 26]) such as, e.g. the investigation of multiphoton ionization in the optical frequency regime [12, 27].

A big advantage of our generic model is that it can be solved analytically. The solution $|\psi\rangle$ of the corresponding Schrödinger equation can be written as

$$|\psi\rangle = \alpha_G\,\mathrm{e}^{-\mathrm{i}(\omega_G+\delta\omega)t}|G\rangle + \alpha_X\,\mathrm{e}^{-\mathrm{i}\omega_X t}|X\rangle + \int_0^\infty \mathrm{d}\omega \sum_\nu \alpha_{\omega\nu}\,\mathrm{e}^{-\mathrm{i}\omega t}|\omega\nu\rangle, \tag{5}$$

where $\delta\omega = \omega_X - \omega_G - \omega_{\mathrm{L}}$ is the detuning of the laser frequency ω_{L} from the transition frequency $\omega_X - \omega_G$ between the resonantly coupled discrete states $|G\rangle$ and $|X\rangle$. Assuming that before switching on the laser the system is in the ground state implies the initial conditions:

$$|\alpha_G| = 1 \quad \text{and} \quad \alpha_X = \alpha_{\omega\nu} = 0 \quad \text{for } t < 0. \tag{6}$$

Inserting the representation (5) into the corresponding Schrödinger equation we obtain for times $t > 0$ the following equations for the coefficients α_G, α_X and $\alpha_{\omega\nu}$:

$$\dot{\alpha}_G = -\mathrm{i}E_0^*\mu_0^*\alpha_X + \mathrm{i}\delta\omega\,\alpha_G, \tag{7a}$$

$$\dot{\alpha}_X = -\mathrm{i}E_0\mu_0\alpha_G - \mathrm{i}\int_0^\infty \mathrm{d}\omega \sum_\nu E_0^*\mu_{\omega\nu}^*\,\mathrm{e}^{\mathrm{i}(\omega_{\mathrm{L}}-\omega+\omega_X)t}\alpha_{\omega\nu}, \tag{7b}$$

$$\dot{\alpha}_{\omega\nu} = -\mathrm{i}E_0\mu_{\omega\nu}\,\mathrm{e}^{-\mathrm{i}(\omega_{\mathrm{L}}-\omega+\omega_X)t}\alpha_X. \tag{7c}$$

Integrating (7c) with the initial condition $\alpha_{\omega\nu} = 0$ for $t < 0$ leads to

$$\alpha_{\omega\nu}(t) = -\mathrm{i}E_0\mu_{\omega\nu}\int_0^t \mathrm{d}t'\,\mathrm{e}^{-\mathrm{i}(\omega_{\mathrm{L}}-\omega+\omega_X)t'}\alpha_X(t'), \tag{8}$$

which can be substituted into (7b) to yield

$$\dot{\alpha}_X = -\mathrm{i}E_0\mu_0\alpha_G - |E_0|^2\int_0^t \mathrm{d}\tau\,\gamma(\tau)\,\alpha_X(t-\tau), \tag{9}$$

$$\text{with} \quad \gamma(\tau) = \int_0^\infty \mathrm{d}\omega \sum_\nu |\mu_{\omega\nu}|^2\,\mathrm{e}^{\mathrm{i}(\omega_{\mathrm{L}}-\omega+\omega_X)\tau}. \tag{10}$$

Thus, eliminating the continuum amplitudes $\alpha_{\omega\nu}$ has led to a closed set of equations for α_G and α_X (cf (7*a*) and (9)) with a memory represented by the function $\gamma(\tau)$. Performing the Laplace transform of (7*a*) and (9) these equations become algebraic and can be solved easily. Recalling the initial conditions (6) the solutions read

$$\alpha_G(s) = \frac{s + |E_0|^2\gamma(s)}{s^2 + |E_0|^2[s\gamma(s) + |\mu_0|^2] - \mathrm{i}\delta\omega[s + |E_0|^2\gamma(s)]}, \tag{11a}$$

$$\alpha_X(s) = \frac{-\mathrm{i}E_0\mu_0}{s^2 + |E_0|^2[s\gamma(s) + |\mu_0|^2] - \mathrm{i}\delta\omega[s + |E_0|^2\gamma(s)]}, \tag{11b}$$

where $\alpha_G(s)$, $\alpha_X(s)$ and $\gamma(s)$ are the Laplace transforms of the time-dependent functions $\alpha_G(t)$, $\alpha_X(t)$ and $\gamma(t)$, respectively.

With (11*a*) and (11*b*) a complete analytical solution of the Schrödinger equation defined by the Hamiltonian in (1) has been constructed in Laplace space, without further approximations. However, in order to understand the physical meaning of this solution it turns out to be instructive to consider the special case of resonant driving of the transition between $|G\rangle$ and $|X\rangle$, i.e. to set $\delta\omega = 0$, and to invoke the widely used Markov approximation. The latter amounts to neglecting the memory in (9), i.e. it is assumed that $\gamma(t)$ decays much faster than the typical time scale on which changes of $\alpha_X(t)$ take place. In this case, we can approximate $\alpha_X(t-\tau) \simeq \alpha_X(t)$ for all values of τ in the integral in (9) where $\gamma(\tau)$ is noticeable different from zero. Thus, in the Markov approximation we neglect the memory effects and write the convolution integrals as

$$\int_0^t \mathrm{d}\tau\, \gamma(\tau)\, \alpha_X(t-\tau) \simeq \int_0^t \mathrm{d}\tau\, \gamma(\tau)\, \alpha_X(t) \simeq \gamma_0\, \alpha_X(t), \tag{12a}$$

$$\text{with} \quad \gamma_0 = \int_0^\infty \mathrm{d}\tau\, \gamma(\tau). \tag{12b}$$

The extension of the upper limit of the integral to infinity in the last step should introduce only a negligible error due to the rapid decay of $\gamma(\tau)$. Within this approximation $\gamma(s)$ in (11) is replaced by the constant γ_0 and the inverse Laplace transformation yields the following analytical expression for the solution for times $t > 0$ in the case $\delta\omega = 0$:

$$\alpha_G(t) = \mathrm{e}^{-\Gamma t}\left[\cos(\Omega t) + \frac{\Gamma}{\Omega}\sin(\Omega t)\right], \tag{13a}$$

$$\alpha_X(t) = -\mathrm{i}\frac{\Omega_0}{\Omega}\,\mathrm{e}^{-\Gamma t}\,\sin(\Omega t), \tag{13b}$$

$$\text{with} \quad \Gamma = \tfrac{1}{2}|E_0|^2\gamma_0, \quad \Omega = \pm\sqrt{|\Omega_0|^2 - \Gamma^2}, \quad \Omega_0 = E_0\mu_0. \tag{13c}$$

We note in passing that the sign of Ω has no effect on α_G and α_X in (13).

The simplicity of (13) allows one to analyze the role of all the contributing processes with ease. First, this solution predicts that the occupations of the two discrete states perform damped Rabi oscillations. The damping of the oscillations is due to the ionization of the atom and its rate is partly determined by Γ in (13*c*). This contribution to the damping rate scales like $\propto |E_0|^2$, which is usually considered as a signature of a single-photon ionization. However, direct single photon ionization of the ground state is impossible in our model and a two-photon process is needed for the ionization in leading order perturbation theory which would result

in a scaling $\propto |E_0|^4$ for the ionization rate. However, this is no contradiction to the results in (13) which reflects the perturbative behavior during the beginning of the first Rabi oscillation where electrons are only transferred from the ground state $|G\rangle$ toward the bound excited state $|X\rangle$ and finally to the continuum, i.e. for times satisfying $\Omega t \ll \pi$. For later times (13) describes an oscillatory exchange of occupation between the bound states $|G\rangle$ and $|X\rangle$ which cannot be captured by low order perturbation theory.

An important prediction of (13) is that the frequency of the Rabi oscillations deviates from its value in the isolated two-level system. It is worthwhile to note that both Γ and Ω in (13) are complex quantities and, therefore, they both contribute to the decay as well as to the renormalization of the oscillation frequency. According to (13*c*) the deviation of Ω from its value $|\Omega_0|$ for the isolated two-level system is expressed explicitly in terms of Γ. Thus, Γ determines both the damping and the frequency renormalization which is the formal expression for the fact that both features have the same physical origin, namely the dipole coupling to the ionization continuum.

Noting that $|\Omega_0|$ and Γ follow different power laws with respect to the field amplitude $|E_0|$ the relative importance of the two contributions to the root $\Omega = \pm\sqrt{|\Omega_0|^2 - \Gamma^2}$ depends on the field strength. In order to further illustrate this fact it is instructive to consider the limiting cases of low, $|\gamma_0 E_0|^2 \ll 4|\mu_0|^2$, and high, $|\gamma_0 E_0|^2 \gg 4|\mu_0|^2$, intensities. In the former case expanding (13*c*) with respect to the small parameter $\lambda = |\gamma_0 E_0|^2/(4|\mu_0|^2)$ gives

$$\Omega \approx \pm\left(|\Omega_0| - \frac{\gamma_0^2}{8}\frac{|E_0|^3}{|\mu_0|}\right), \tag{14}$$

i.e. for low intensities the shift of the Rabi frequency scales like $\propto |E_0|^3$. Following (13*c*) the leading order of the damping rate is $\propto |E_0|^2$, while the next order correction is obtained by taking the imaginary part of (14), which gives a correction $\propto |E_0|^3$. One can see that in this limit, larger field intensities lead to a stronger ionization as well as to a larger renormalization of the Rabi frequency. A similar dependence on the dipole couplings to the continuum follows from equations (10), (12*b*) and (13*c*), namely an increase in the coupling constants $\mu_{\omega\nu}$ leads to larger damping rates and frequency shifts.

In the opposite limit of high intensities we obtain from (13*c*) by keeping the leading and next to leading order contributions in an expansion with respect to $1/\lambda$:

$$\Omega \approx \pm\mathrm{i}\left(\Gamma - \frac{|\mu_0|^2}{\gamma_0}\right). \tag{15}$$

Substituting (15) into (13*a*) we find asymptotically for large $|E_0|$ the prediction

$$\alpha_G(t) \approx \mathrm{e}^{-\frac{|\mu_0|^2}{|\gamma_0|^2}\gamma_0^* t}, \tag{16}$$

i.e. the dynamics of the ground state occupation loses its oscillatory character, becoming a monotonically decaying function with a rate that is independent on the intensity. Therefore, equations (13) predict a saturation of the intensity dependences at larger fields.

3. Numerical results

The generic model developed so far applies to many specific situations as many different atomic systems support Rabi oscillations between two discrete states in competition to single photon ionization from the upper level. In this section we shall discuss specifically the case of a model

system with two laser driven electrons in an atomic potential that exhibits two bound states which can be resonantly coupled by the laser, i.e. a situation where the results of our generic model are supposed to be applicable. The purpose of this discussion is twofold. Firstly, we would like to illustrate the intensity dependence of the ionization and the accompanying shift of the Rabi frequency. Currently, e.g. at FLASH intensities of the order $\approx 10^{13}$–$10^{14}\,\mathrm{W\,cm^{-2}}$ are used in experiments [28, 29] while measurements at the Linac Coherent Light Source are reported with $I \approx 10^{16}\,\mathrm{W\,cm^{-2}}$ [30]. Intensities of the same order have also been reached by the FERMI FEL in Trieste where recently the first operation with externally seeded, longitudinally coherent XUV pulses has been reported [24].

We have simulated a range of intensities starting at the low end at about $\approx 10^{10}\,\mathrm{W\,cm^{-2}}$ and going up to values between $\approx 10^{15}\,\mathrm{W\,cm^{-2}}$ and $\approx 10^{16}\,\mathrm{W\,cm^{-2}}$. Thus, our simulations cover a range of intensities that is typical for current experiments. Second, the approximations implicit in the formulation of the Hamiltonian (1), that were needed in order to have a generic model that is analytically solvable, will be abandoned here. Comparing full numerical results with calculations along the lines of the previous section enables us to discern the strengths and weaknesses of the analytical results found above.

3.1. Non-interacting electrons

At first we shall neglect the interaction between the electrons and in order to further reduce the numerical complexity we concentrate on one space dimension. This model is simple enough to allow for a full numerical treatment as well as for the calculation of all energies and matrix elements needed in order to perform calculations based on our analytical formulae. With these assumptions the Hamiltonian for this model can be written in real space as

$$H_\mathrm{e} = \sum_{j=1}^{2} H_\mathrm{s}(x_j) \tag{17}$$

with the single particle Hamiltonian

$$H_\mathrm{s}(x) = -\frac{\hbar^2}{2m}\frac{\partial^2}{\partial x^2} + V(x) + e\,E(t)\,x, \tag{18}$$

where m is the electron mass. For the atomic potential we choose

$$V(x) = \frac{-V_0}{\sqrt{x^2+\kappa^2}}, \tag{19}$$

which is widely used in the literature [7, 31][4]. Usually, one-dimensional models are considered in order to obtain a simple model where the interaction between the electrons can also be accounted for. For such a system, a standard way to fix the parameters V_0 and κ is to identify V_0 with the core charge Z, which guarantees the same asymptotic for $|x| \to \infty$ as in the three-dimensional case and to set $\kappa = 1$ in atomic units, which removes the singularity on the scale of the core radius. In order to facilitate the comparison of calculations, where we neglect the electron–electron interaction, with the interacting system, we have adjusted the parameters V_0 and κ in the former case such that the ground state energy and the first ionization potential are similar to those derived with interaction and the standard choice of parameters.

[4] In our calculations we also make use of the *complex absorbing potential* approach in order to realize absorbing boundaries [32].

This is achieved by setting $V_0 = 1.8 R_Y a_{Bohr}$ and $\kappa = 0.73 a_{Bohr}$, with R_Y being the Rydberg constant and a_{Bohr} the Bohr radius. The energies of the two orbitals with lowest energies of the corresponding stationary single electron Schrödinger equation then turn out to be $E_G = -21$ eV and $E_X = -7$ eV, respectively. It should be noted, that different from the assumption in our generic model this potential supports a Rydberg like series of bound states [31] in addition to the two lowest states.

The laser field is taken to be the one-dimensional analogue of $\vec{E}(t)$ in (3), i.e.

$$E(t) = \theta(t)\, E_0\, \mathrm{e}^{-\mathrm{i}\omega_L t} + \mathrm{c.c.} \tag{20}$$

As the electrons are non-interacting the two-electron wave function ψ is a single Slater-determinant for all times. Assuming that the system is initially in the ground state it is given by the singlet state

$$\psi(x_1,\sigma_1; x_2,\sigma_2,t) = \varphi(x_1,t)\varphi(x_2,t)\frac{(\delta_{\sigma_1\uparrow}\delta_{\sigma_2\downarrow} - \delta_{\sigma_2\uparrow}\delta_{\sigma_1\downarrow})}{\sqrt{2}}. \tag{21}$$

Here, the orbital $\varphi(x,t)$ solves the single particle time-dependent Schrödinger equation (TDSE)

$$\mathrm{i}\hbar\dot{\varphi}(x,t) = H_s(x)\varphi(x,t) \tag{22}$$

with the initial condition $\varphi(x,t)|_{t=0} = \varphi_G(x)$, where φ_G is the single particle ground state wave function. Expanding $\varphi(x,t)$ in the eigenbasis of H_s yields equations of motion for the coefficients that can be reduced to (7) when four approximations are made: (i) direct dipole couplings from the ground state to the continuum are neglected, (ii) dipole couplings between continuum states are disregarded, (iii) only the two lowest bound states are kept and (iv) the RWA is applied. Thus, by calculating all remaining dipole matrix elements we are able to construct the memory function $\gamma(\tau)$ (cf (10)) for the present model and from this we can derive the parameter γ_0 (cf (12*b*)), which in turn fully determines the solution in the Markov approximation given in (13). The comparison of results derived in this way from (13) with a direct numerical solution of (22) in real space will therefore provide insights into the role of the approximations (i)–(iv) combined with the Markov approximation. As a further option, with $\gamma(\tau)$ at hand we can avoid the Markov approximation and fully account for the memory by solving directly (7*a*) and (9). This allows us to separate the influences of the approximations (i)–(iv) from the impact of the Markov approximation.

Shown in figure 2 is the occupation of the two-electron ground state for three different intensities as a function of time. Results of a direct numerical solution of (22) in real space (blue solid lines) are compared with calculations where the approximations (i)–(iv) are invoked (red dashed dotted lines or circles). Also shown are curves representing the Markov limit of the latter (green dotted lines or crosses).

At an intensity of $I = 3.52 \times 10^{12}\,\mathrm{W\,cm^{-2}}$ (figure 2(a)), all three levels of the theory give practically the same result, namely weakly damped Rabi oscillations with essentially a single frequency. Increasing the intensity to $I = 1.27 \times 10^{14}\,\mathrm{W\,cm^{-2}}$ (figure 2(b)) the oscillations are faster and the damping is stronger, as expected. Although the results of the three different simulations are still very close to each other, first deviations of the two approximate simulations from the full numerical solution are visible, while the Markov approximation seems to have still little impact at this intensity. Only when the intensity is further increased to $I = 1.41 \times 10^{15}\,\mathrm{W\,cm^{-2}}$ (figure 2(c)) the Markov approximation predicts systematically a weaker damping, i.e. less ionization, and faster oscillations than calculations that keep the memory.

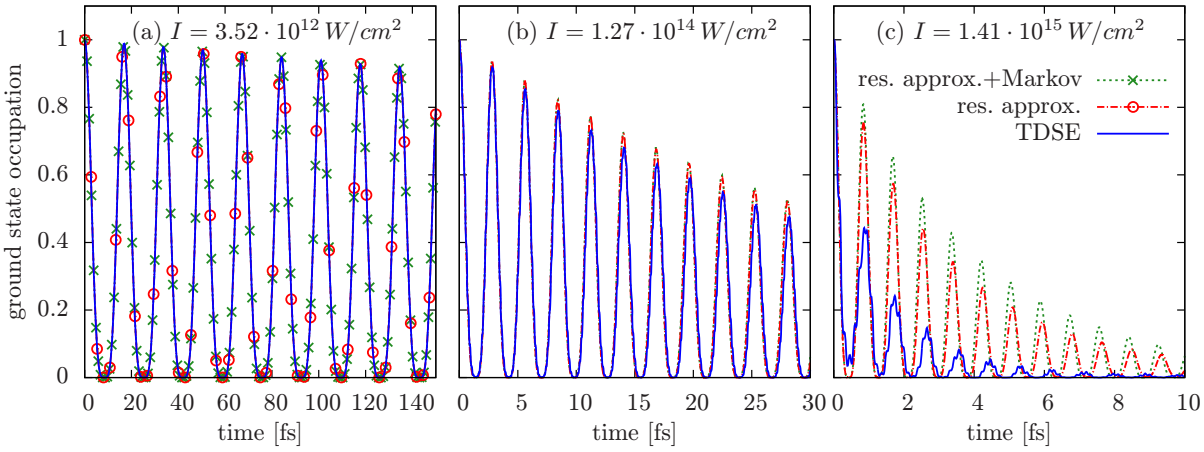

Figure 2. Ground state occupation for a system of two non-interacting electrons calculated for three intensities I as indicated and different levels of the theory: full numerical solution of the Schrödinger equation (blue solid line), using the generic model where only resonant contributions to the dynamics are kept (red dashed dotted line or circles) and applying the Markov approximation to the latter, i.e. using (13*a*) (green dotted line or crosses).

It is remarkable, however, that both approximate approaches deviate much less from each other than from the full solution. The ionization derived from the latter is much stronger and also the frequency is noticeably lower. In addition, high frequency modulations show up in the full solution that are superimposed on the decaying Rabi oscillation. These additional modulations are due to the parts of the laser driving that are neglected in the RWA. In the rotating frame associated with the Bloch sphere of the two discrete levels these parts provide an off-resonant driving with twice the laser frequency which at high intensities gives rise to fast modulations on top of the Rabi flops.

Finally, we note that although our analytically solvable model captures qualitatively most of the features of the full numerical solution, quantitatively it comes to its limits of validity before reaching the high intensity regime, where according to (16) the ground state occupation should exhibit an intensity independent decay without oscillations. Obviously, the processes neglected by the approximations (i)–(iv) have a noticeable impact at elevated intensities. Direct off-resonant dipole couplings from the ground state to the continuum (neglected in approximation (i)) will increase the ionization. The main effect of couplings within the continuum is to promote electrons that have been transferred by the laser to states less than one photon energy $\hbar\omega_{\mathrm{L}}$ above the continuum threshold to higher energies. This reduces the Pauli blocking for subsequent single ionization processes and also reduces the recapture probability. Therefore, also using approximation (ii) will lead to a reduction of the resulting ionization. Keeping all bound states opens further off-resonant ionization channels. Thus, approximation (iii) reduces the ionization as well. Finally, the RWA (approximation (iv)) suppresses the fast modulations seen in the full simulation and also neglects some off-resonant ionization channels. These considerations qualitatively explain the tendencies seen in figure 2(c). It is, however, remarkable how strong the increase of the ionization due to off-resonant processes actually is although here we have considered Fourier-limited excitations that are spectrally narrow compared with SASE pulses of the same duration.

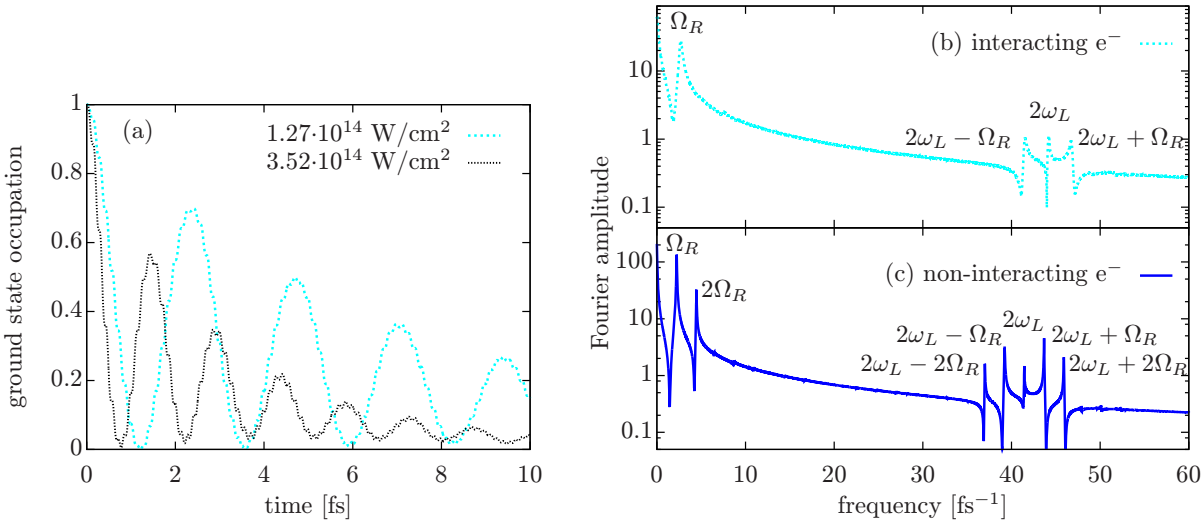

Figure 3. (a) Ground state occupation for a system of two interacting electrons calculated by a full numerical solution of the Schrödinger equation for two intensities I as indicated. (b) Fourier transform of the curve in (a) for $I = 1.27 \times 10^{14}\,\mathrm{W\,cm^{-2}}$. Panel (c) same as (b) but calculated without electron–electron interaction.

3.2. Interacting electrons

It will turn out to be instructive to compare the dynamics of non-interacting electrons with simulations where the electron–electron interaction is accounted for. For a system of two one-dimensional electrons such simulations are easily done by adding the potential

$$-\tfrac{1}{2}V(x_1-x_2) \tag{23}$$

to the Hamiltonian H_e in (17) and solving numerically the corresponding two-dimensional Schrödinger equation. For calculations with electron–electron interaction we shall use the standard parametrization of the potential [7, 31] discussed before, i.e. we set $V_0 = 2$ and $\kappa = 1$ in atomic units.

At first sight, the ground state dynamics with and without electron–electron interaction are very similar as can be seen by comparing the results without interaction in figure 2 with corresponding curves where the interaction has been taken into account in figure 3(a). Also in the latter case, we see damped Rabi oscillations where with rising intensity the damping increases and the oscillations become faster. The intensities used for the simulation shown in figure 3(a) are high enough that the fast modulations due to non-RWA contributions to the dynamics are clearly visible.

A more detailed picture is obtained by taking the Fourier transform of these time traces. These are displayed in figures 3(b) and (c) and reveal rich spectra that differ for interacting and non-interacting calculations. In both cases there is a single dominant peak in the spectrum which corresponds to the main oscillation in the time domain. We shall refer to the corresponding frequency as the Rabi frequency and denote it by Ω_R. The different values for Ω_R with and without interaction reflect the change of the dipole matrix element for the transition between the bound states when the interaction is accounted for. The spectra exhibit further features at

twice the laser frequency ω_L with satellites at $2\omega_L \pm \Omega_R$. These features stem from non-RWA type contributions. Interestingly, the spectrum calculated without electron–electron interaction comprises an additional peak at $2\Omega_R$ and additional satellites at $2\omega_L \pm 2\Omega_R$. Formally, these extra peaks arise because the two-electron wave function without interaction is a product of single particle wave functions $\varphi(x,t)$ (cf (21)). Therefore, the occupation of the ground state of the two-electron system is given by $|\alpha_G^{(s)}(t)|^4$, where $\alpha_G^{(s)}$ is the projection of $\varphi(x,t)$ on the single particle ground state $\varphi_G(x)$. As the dynamics of $\alpha_G^{(s)}$ is of the type discussed within our generic model for the amplitude α_G, taking the fourth power of $|\alpha_G^{(s)}(t)|$ instead of the square, brings in the higher harmonics of Ω_R. In order to understand why these higher harmonics are absent when the electron–electron interaction is present, we recall that the product structure of the two-particle wave function in (21) expresses the fact that the two electrons evolve independently under the action of the laser. In particular, this implies that the wave function comprises contributions where both electrons are in the upper excited single particle state, which is a localized state. However, the energy for promoting both electrons into the upper discrete state is higher than the energy needed for a single electron ionization. Thus, in a system with electron–electron interaction an excitation with two localized electrons with an energy above the ionization threshold cannot be stable and consequently dissolves as part of the ionization continuum. As a consequence, in the system with interaction it is the two-particle state that is well represented in the form given by (5) while without interaction this representation applies to the single particle wave function $\varphi(x,t)$ which according to (21) enters the two-particle wave function twice as a factor. Therefore, with interaction the ground state occupation essentially behaves like the square of the absolute value of the generic amplitude α_G in (13*a*) while without interaction it enters in the fourth power.

In order to quantify the intensity dependence of the Rabi frequency we have calculated spectra as shown in figures 3(b) and (c) for different intensities and extracted Ω_R. We have also determined the full-width-at-half-maximum Γ_R of the peak at Ω_R as a measure of the decay of the Rabi oscillations. Γ_R and Ω_R are displayed in figure 4 as functions of the intensity for calculations with and without electron–electron interaction. As a further comparison we have extracted the same quantities for the analytical model corresponding to non-interacting electrons both with and without Markov approximation. In all cases Γ_R rises almost strictly linearly with intensity over a large intensity range. Within the Markov limit of our generic model (cf (13)) we have found that according to (16) this rise should eventually saturate at high intensities. However, instead of a saturation we find from figure 4 that the solution of the Schrödinger equation predicts a damping that actually rises super-linearly. Also, when the Markov approximation is not invoked in our solvable model a tendency for a stronger than linear increase of Γ with intensity is found, which is, however, not as pronounced as in the full solution of the Schrödinger equation. Only the Markovian result still rises almost linearly with I over the whole studied intensity range which is in accordance with the expansion (14) as the smallness parameter λ is even at $I = 10^{15}\,\mathrm{W\,cm^{-2}}$ still below 1%. Figure 4 also nicely illustrates that the increasing ionization is accompanied by a larger deviation of the Rabi frequency from its value $|\Omega_0|$ for an isolated two-level system. With and without interaction we find a reduction of the Rabi frequency which for the interacting system and intensities of the order of $I \gtrsim 10^{15}\,\mathrm{W\,cm^{-2}}$ reaches only $\sim$75% of its unrenormalized value. It turns out that the dipole coupling to the continuum is stronger for the interacting system and thus we find a larger ionization than in simulations without electron–electron interaction. The fact, that in accordance with our analysis for the generic model also the shift of the Rabi frequency is larger with than without interaction,

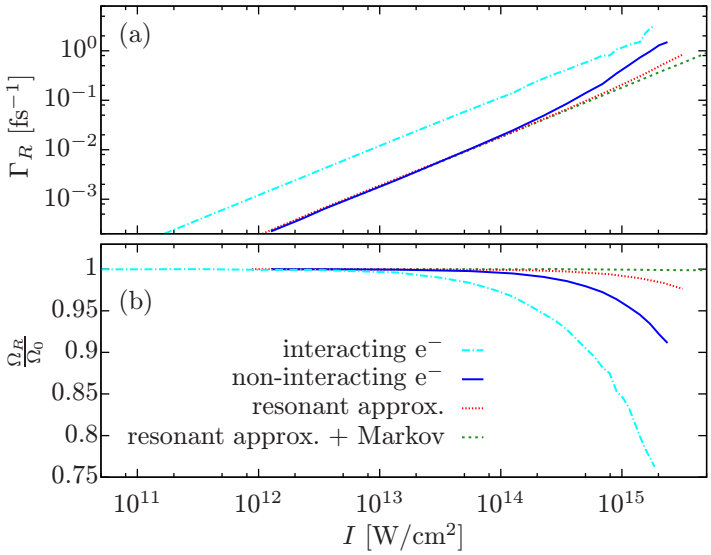

Figure 4. (a) Damping and (b) effective frequency of the Rabi-oscillations normalized to the Rabi frequency of an isolated two-level system $|\Omega_0|$ as a function of the intensity I for a two electron system with (light blue dashed dotted lines) or without (blue solid lines) electron–electron interaction, using the generic model for the non-interacting case that keeps only resonant contributions (red dotted lines) and applying the Markov approximation to the latter (green dashed lines).

corroborates our conclusion that the ionization strength and the magnitude of the shift are related because both arise from the same physical mechanism, i.e. the coupling of the upper discrete state to the ionization continuum. We find over the whole range of intensities studied here that both the damping and the shift exhibit in parallel a monotonic non-saturating increase that persists also for high intensities that are out of the range of validity of the generic model. Interestingly, the magnitude of the shift is strongly enhanced by non-Markovian parts of the dynamics as well as by off-resonant contributions. Indeed, the shift predicted by our analytical model in the Markov limit is hardly visible on the scale shown in figure 4. Abandoning the Markov approximation it becomes noticeable and accounting in addition for off-resonant parts of the dynamics it acquires a remarkable size, especially in the case with electron–electron interaction.

3.3. Impact of Rabi oscillations on the ionization dynamics

Transferring electrons back and forth between discrete localized levels—as done in a Rabi oscillation—does, of course, not directly contribute to the ionization, because the carriers that stay in the Rabi cycle do not leave the atom. Nevertheless, the ionization is affected by Rabi oscillations as it is much easier for an electron to escape the atom from the upper than from the lower level. In order to illustrate this effect we have calculated the ionization probability P_I by identifying

$$P_\mathrm{I} = 1 - P_\mathrm{bound}, \tag{24}$$

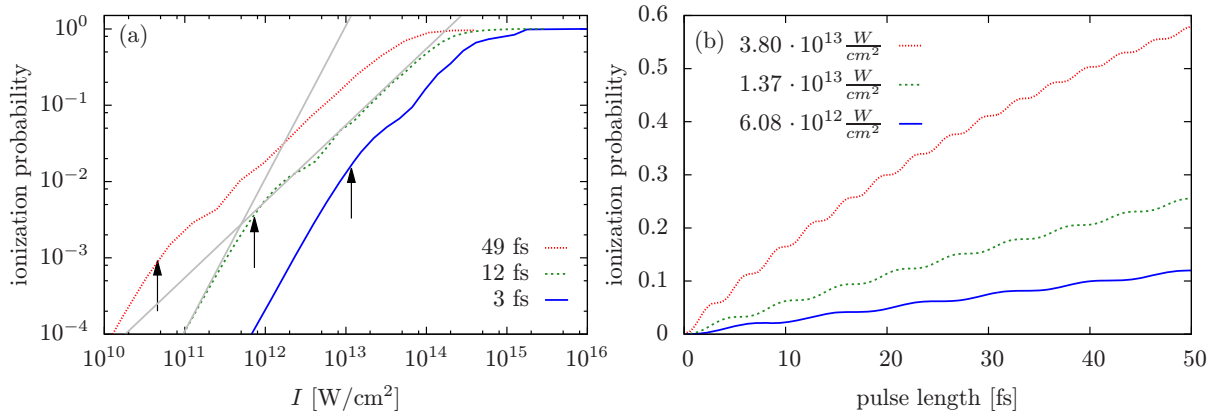

Figure 5. Ionization probability of a system of two non-interacting electrons: (a) for three pulse durations as a function of the intensity I and (b) for three intensities as a function of the pulse length. Gray lines mark in (a) a strict linear or quadratic intensity scaling as a reference, while arrows indicate the intensity corresponding to a pulse area of $A = \pi$.

where P_{bound} is the total probability to occupy one of the localized bound states after the laser excitation has ended. Here, a two-electron state is counted as bound, when both electrons are localized to the atom[5], i.e. P_{I} includes the ionization probability for single and double ionization. Plotted in figure 5(a) is P_{I} versus the intensity for three different pulse durations. The calculations have been performed for the model of two non-interacting electrons introduced in section 3.1.

For high enough intensities we observe that P_{I} grows almost linearly with intensity until it eventually saturates. Such a linear scaling has also been measured in recent experiments on the single ionization of He where the photon energy covered the 1s2p and 1s3p resonant transitions [33]. At these intensities the ionization reflects the escape of carriers from the atom averaged over one or more Rabi cycles. This loss gives rise to the damping of the Rabi oscillation that has been shown in the previous subsections to scale linearly with intensity. The linear scaling manifests the fact that in each Rabi cycle the main flow of carriers away from the atom occurs when the atom occupies the upper discrete state from which the ionization can take place as a single photon process. Here, the Rabi oscillation between the two resonantly driven states provides over a cycle an average occupation of the upper level from which the single photon ionization can start. Averaged over a cycle the Rabi flops do, however, not introduce a significant modification of the intensity scaling.

In contrast, when the intensity is lowered such that within the duration τ_{pulse} of the pulse less than the first half cycle is completed, i.e. when the pulse area $A = \Omega_{\text{R}}\tau_{\text{pulse}} < \pi$, then the occupation of the upper level rises monotonically with intensity. As a result the observed ionization being a two-step process composed of the Rabi rotation to the upper level followed by the single photon ionization exhibits an intensity scaling that is affected by both of these partial processes. This can also be seen explicitly within our generic model where the low laser power behavior can be obtained by calculating P_{I} with the help of the solution (13) and expanding the

[5] For non-interacting electrons this condition coincides with the requirement that both electrons occupy a bound single electron state.

result with respect to E_0. In this way it is easily verified that at low intensities P_I scales like $\propto I^2$. Indeed, comparing with a strict quadratic scaling (indicated as a gray line in figure 5(a)) it is seen that our numerical results for P_I follow the quadratic rise to a good approximation almost up to the intensity that corresponds to the pulse area $A = \pi$ (marked by arrows in figure 5(a)). A similar crossover from a quadratic to an almost linear scaling of P_I has been found previously for a discrete three-level model where a complex valued energy has been assigned to the uppermost state to simulate the particle escape from the atom [18]. Within this model simulations have been presented in [18] for a fixed pulse duration. The interpretation that the regime of linear scaling should be reached when one or more Rabi cycles are completed within the duration of the pulse suggests that the crossover between quadratic and linear scaling should depend crucially on the pulse length. This is, indeed, seen in figure 5(a). It is also worthwhile to note that while in an isolated two-level system the pulse length τ_{pulse} and the amplitude E_0 enter the resonant Rabi signal not independently but only via the pulse area $A = |\mu_0 E_0|\tau_{\text{pulse}}$, this is no longer true here as can be seen, e.g. from the solution (13). As a consequence, the intensity dependent signals plotted in figure 5(a) for different pulse durations are not just rescaled curves of identical shape (as would be true for an isolated two-level system). By varying τ_{pulse} and I as independent parameters it is thus possible to control to some extend the interplay between the ionization process and the Rabi oscillation.

Figure 5 also reveals that superimposed on the approximate power law behavior are modulations that obviously result from the non-monotonic variation of the occupation of the upper resonantly coupled bound state due to the Rabi oscillations. More direct access to the Rabi oscillations can be obtained by extracting the ionization probability for fixed intensities as a function of the pulse duration. As seen in figure 5(b) such signals exhibit clear modulations with the Rabi frequency Ω_R and thus in principle allow for an extraction of Ω_R from ionization signals. The ionization increases steeply during time intervals where the upper bound state is significantly occupied while only little extra ionization takes place otherwise.

Before closing, we would like to emphasize that our generic analysis is not restricted to the one-dimensional models that we have used for illustration purposes. We therefore expect that generic features such as the shift of the Rabi frequency or the pulse duration dependent crossover from a quadratic to a linear intensity scaling of the ionization probability should occur also in realistic three-dimensional models where two resonantly driven discrete states are exposed to photoionization.

4. Conclusions

We have theoretically investigated the dynamics of systems where two discrete atomic states are resonantly coupled by a strong coherent laser field that in addition to driving the transition between these states can also ionize the atom. The competition between Rabi oscillations and ionization leads to pronounced differences compared with both the Rabi oscillations within an isolated two-level system and the ionization without the resonantly coupled intermediate level. The ground state occupation is shown to exhibit damped Rabi oscillations. The damping turns out to increase almost linearly with the laser intensity over a wide intensity range. The increase of the damping with rising intensity is shown to be accompanied by a shift of the Rabi frequency compared with its value for an isolated two-level system, which also increases with increasing intensity.

The damping and the frequency renormalization are both due to the coupling of the two discrete levels to the ionization continuum. Being of the same physical origin provides a close relation between these features which was explicitly derived within a simplified analytically solvable model. Comparing the analytical results with numerical simulations for a two-electron system revealed for high intensities the importance of off-resonant couplings that were neglected in the simplified model. Furthermore, also the Markov approximation is shown to come to its limits at elevated intensities and often neglected memory effects gain in importance. In addition, simulations with and without electron–electron interactions demonstrate a qualitative impact of the interaction on the dynamics that manifests itself in additional harmonics of the Rabi-frequency in the time evolution of the ground state occupation that occur when the interaction is neglected. The simulations also demonstrate that the qualitative behavior of the damping and the frequency renormalization with respect their intensity dependences is practically not affected by the interaction.

Finally, the ionization probability is shown to exhibit a pulse length dependent crossover from a quadratic intensity scaling that would be expected from perturbative arguments for a two-photon ionization to an almost linear intensity dependence. The crossover sets in roughly when one or more Rabi cycles can be completed within the pulse duration. The simulations suggest that features like the shift of the Rabi frequency or the crossover in the intensity scaling of the ionization probability are generic features of ionization processes that proceed via a resonantly driven intermediate level.

Acknowledgments

We gratefully acknowledge the financial support by the Bundesministerium für Bildung und Forschung BMBF through the grants 05K10WCA and 05K10PSB. We also acknowledge stimulating discussions with I D Feranchuk and D Hochstuhl.

References

[1] Richter M, Amusia M Y, Bobashev S V, Feigl T, Juranić P N, Martins M, Sorokin A A and Tiedtke K 2009 *Phys. Rev. Lett.* **102** 163002
[2] Rohringer N and Santra R 2009 *Phys. Rev.* A **79** 053402
[3] Young L *et al* 2010 *Nature* **466** 56
[4] Doumy G *et al* 2011 *Phys. Rev. Lett.* **106** 083002
[5] Kaiser B, Vagov A, Axt V M and Pietsch U 2011 *Phys. Rev.* A **84** 043431
[6] Rudek B *et al* 2012 *Nature Photon.* **6** 858
[7] Ruiz C, Plaja L and Roso L 2005 *Phys. Rev. Lett.* **94** 063002
[8] Lorenz U, Kabachnik N M, Weckert E and Vartanyants I A 2012 *Phys. Rev.* E **86** 051911
[9] Makris M G, Lambropoulos P and Mihelič A 2009 *Phys. Rev. Lett.* **102** 033002
[10] Son S K, Chapman H N and Santra R 2011 *Phys. Rev. Lett.* **107** 218102
[11] Thiele R, Son S K, Ziaja B and Santra R 2012 *Phys. Rev.* A **86** 033411
[12] Beers B L and Armstrong L 1975 *Phys. Rev.* A **12** 2447
[13] Knight P L 1977 *Opt. Commun.* **22** 173
[14] Demekhin P V and Cederbaum L S 2012 *Phys. Rev. Lett.* **108** 253001
[15] Galayda J N, Arthur J, Ratner D F and White W E 2010 *J. Opt. Soc. Am.* B **27** B106
[16] McNeil B W J and Thompson N R 2010 *Nature Photon.* **4** 814
[17] Palacios A, Bachau H and Martin F 2006 *Phys. Rev.* A **74** 031402

[18] Sako T, Adachi J, Yagishita A, Yabashi M, Tanaka T, Nagasono M and Ishikawa T 2011 *Phys. Rev.* A **84** 053419
[19] Liao Q, Zhou Y, Huang C and Lu P 2012 *New J. Phys.* **14** 013001
[20] Rohringer N and Santra R 2008 *Phys. Rev.* A **77** 053404
[21] Rohringer N and Santra R 2012 *Phys. Rev.* A **86** 043434
[22] Demekhin P V and Cederbaum L S 2011 *Phys. Rev.* A **83** 023422
[23] Kanter E P *et al* 2011 *Phys. Rev. Lett.* **107** 233001
[24] Allaria E *et al* 2012 *Nature Photon.* **6** 699
[25] Coleman P E and Knight P L 1981 *J. Phys. B: At. Mol. Phys.* **14** 2139
[26] Kyrola E 1986 *J. Phys. B: At. Mol. Phys.* **19** 1437
[27] Popescu D, Collins C B, Johnson B W and Popescu I 1974 *Phys. Rev.* A **9** 1182
[28] Chapman H N *et al* 2007 *Nature* **448** 676
[29] Krikunova M *et al* 2012 *J. Phys. B: At. Mol. Opt. Phys.* **45** 105101
[30] Chapman H N *et al* 2011 *Nature* **470** 73
[31] Su Q and Eberly J H 1991 *Phys. Rev.* A **44** 5997
[32] Vibok A and Balintkurti G G 1992 *J. Phys. Chem.* **96** 8712
[33] Sato T *et al* 2011 *J. Phys. B: At. Mol. Opt. Phys.* **44** 161001